CrystEngComm

Accepted Manuscript

ROYAL SOCIETY OF CHEMISTRY

www.rsc.org/crystengcomm

Journal Name

RSCPublishing

COMMUNICATION

Cite this: DOI: 10.1039/x0xx00000x

Diethylenetriamine-Assisted Hydrothermal Synthesis of Dodecahedral α-Fe_2O_3 Nanocrystals with Enhanced and Stable Photoelectrochemical Activity

Rui Xu, You Xu, Yi Huang, Yanmei Shi and Bin Zhang*

Received 00th January 2012,
Accepted 00th January 2012

DOI: 10.1039/x0xx00000x

www.rsc.org/

Dodecahedral α-Fe_2O_3 nanocrystals (D-hematite) were successfully synthesized through a hydrothermal method involving FeS-diethylenetriamine (FeS-DETA) hybrid nanosheets as starting materials. The photoanode made by assembling the as-obtained D-hematite on ITO substrates exhibited efficient photoelectrocatalytic water splitting activity and good stability in 1.0 M KOH aqueous solution under visible light irradiation.

1.Introduction

Photoelectrochemical (PEC) water splitting is an environmentally friendly and promising approach for converting solar energy into chemical energy.[1-3] The pioneering work was published by Fujishima and Honda in 1972, in which "Honda–Fujishima effect" and photoelectrolysis using n-type TiO_2 as the photoelectrode were first described.[4] A plenty of PEC materials, especially semiconductor oxides[5-10], have been investigated. As a typical example, hematite (α-Fe_2O_3) is considered as one of the most promising candidates for visible-light-driven PEC water splitting due to its abundance, low cost, non-toxicity, excellent stability and appropriate band positions for visible light absorption.[11-15] However, poor mobility of photogenerated carriers, short hole diffusion length and slow oxidation kinetics limit the performance of α-Fe_2O_3 in the PEC water splitting.[16-21] Therefore, it is necessary to develop facile and cost-effective methods to synthesize active α-Fe_2O_3 for PEC water splitting.

Intensive researches have been done to explore the synthesis of nanostructured α-Fe_2O_3,[22-26] such as nanoparticles,[27-29] nanorods/nanowires,[30-33] nanotubes,[34] nanoplates/nanosheets,[35-38] nanoflowers[39,40] and nanocubes,[41-45] owing to their larger active surface areas, better light absorption, and increased photocurrent compared with the corresponding bulk counterparts. However, the synthesis of nanostructured α-Fe_2O_3 polyhedrons still remain challenging because polyhedral metal oxides have more complex crystal systems than metal nanocrystals.[46-52] To date, only a few excellent reports have been done on the preparation of polyhedral α-Fe_2O_3 nanocrystals. For example, Gao group and Wang group established a solvothermal method to prepare tetrakaidecahedral and oblique parallelepiped hematite in the presence of carboxymethyl cellulose (CMC) and poly(vinylpyrrolidone) (PVP).[53,54] Lv *et al.* reported an efficient fabrication of dodecahedral and octadecahedral α-Fe_2O_3 in the existence of fluoride anions.[55] Meanwhile, the present applications of polyhedral α-Fe_2O_3 are mainly focused on the magnetic measurements[56,57]and gas-sensing properties[58,59]. Thus, it is highly desirable to develop a facile strategy to fabricate single-crystalline polyhedral α-Fe_2O_3 for the PEC water splitting.

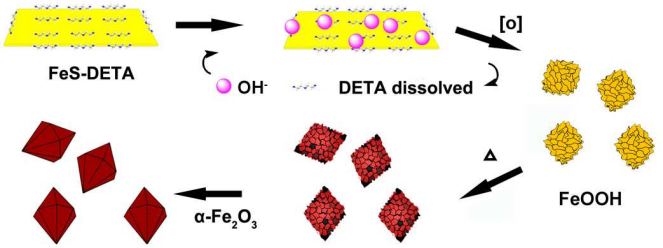

Scheme 1 Scheme illustrating for the preparation of single-crystalline dodecahedral α-Fe_2O_3 through the anion-exchange reaction of the organic-inorganic FeS-DETA hybrid nanosheets with OH^- at elevated temperature.

Herein, we reported the synthesis of single-crystalline dodecahedral α-Fe_2O_3 through a facile hydrothermal approach.

The simple protocol involved the use of inorganic-organic hybrid FeS-amine nanosheets as the starting material, the mixture of amine and water as solvent and reaction agent (Scheme 1). It was found that the choice of amine was crucial to the formation of dodecahedral morphology. And the dissolution of amine facilitated the reaction process. Furthermore, the as-prepared dodecahedral α-Fe_2O_3 nanocrystals exhibited efficient PEC water splitting activity and good stability under visible light irradiation (λ> 420 nm), compared with commercial α-Fe_2O_3. Traditionally, to achieve efficient PEC water splitting activity, the α-Fe_2O_3 is mainly synthesized using deposition technique at high temperature (spray pyrolysis and CVD,400-500°C) or solution-based methods with following annealing steps (700-800°C).[12] However, in our experiments, photoactive dodecahedral α-Fe_2O_3 nanocrystals were prepared at a low temperature (200°C) using hydrothermal method. The photocurrent density of dodecahedral α-Fe_2O_3 nanocrystals is 3.06 mA cm^{-2} at the potential of 1.6V versus RHE under visible light illumination (λ > 420 nm). To the best of our knowledge, this value is comparable or even higher than most of ever measured undoped hematite films without any cocatalysts (Table S1).

2. Experimental section

2.1 Materials

All chemicals are analytical grade and used as received without further purification.

2.2 Synthesis of inorganic-organic hybrid FeS-DETA nanosheets

FeS-DETA was synthesized using a modified method reported by the Yu's group.[55,56] In a typical synthesis procedure, $FeSO_4 \cdot 7H_2O$ (0.2780 g), C_2H_5NS (0.1526 g), H_2O (8 mL) and diethylenetriamine (DETA, 8 mL) were added to a Teflon-lined autoclave with a capacity of 20 mL. The mixture was stirred for 20 min to form a homogeneous suspension. The autoclave was then sealed and heated at 140 °C for 24 h. After reaction, the autoclave was cooled down to room temperature naturally. In our manuscript, the hybrid nanosheets are named as FeS-DETA.

2.3 Synthesis of dodecahedral α-Fe_2O_3

In a typical procedure, the as-obtained inorganic-organic hybrid FeS-DETA nanosheets were vigorously stirred for 30 min to form a homogeneous suspension. Then the as-obtained dispersions (0.8 mL) were centrifuged at 12000 rpm for 3 min to remove the supernatant transparent solution which may contain the redundant reagent. After centrifugation, the dispersions were diluted with 11.0 mL H_2O and 0.1 mL DETA. Then the mixture was added to a Teflon-lined autoclave with a capacity of 20 mL and heated at 200 °C for 6 h. After cooling to room temperature, the precipitate was collected by centrifugation and washed with ethanol for three times. The final product was dried in a vacuum oven at room temperature for 6 h.

2.4 Photoelectrochemical Measurements

Photoelectrochemical measurements were carried out in a standard three-compartment cell consisting of a working electrode, a Pt sheet counter electrode, and a Hg/HgO (1.0 M KOH) reference electrode performed using an electrochemical workstation (CHI 660D, CH Instruments, Austin, TX) under a 300 W Xe lamp equipped with a 420 nm cut-off filter. The solution of 1.0 M KOH (pH=13.6) was employed as electrolyte. Oxygen was purged from the electrolyte using bubbled nitrogen gas. An indium-tin oxide glass (ITO) decorated with catalyst samples were used as the working electrode. For a typical procedure for fabricating the working electrode, 1 mg of α-Fe_2O_3 catalysts were dispersed in solution containing water (0.5 mL), CH_3CH_2OH (0.5 mL) and 5 wt% Nafion solution (10 μL) then the mixture was ultrasonicated to generate a homogeneous ink. Then 160 μL of the catalyst ink was spreaded on an ITO glass (loading amount: ~ 0.158 mg cm^{-2}).

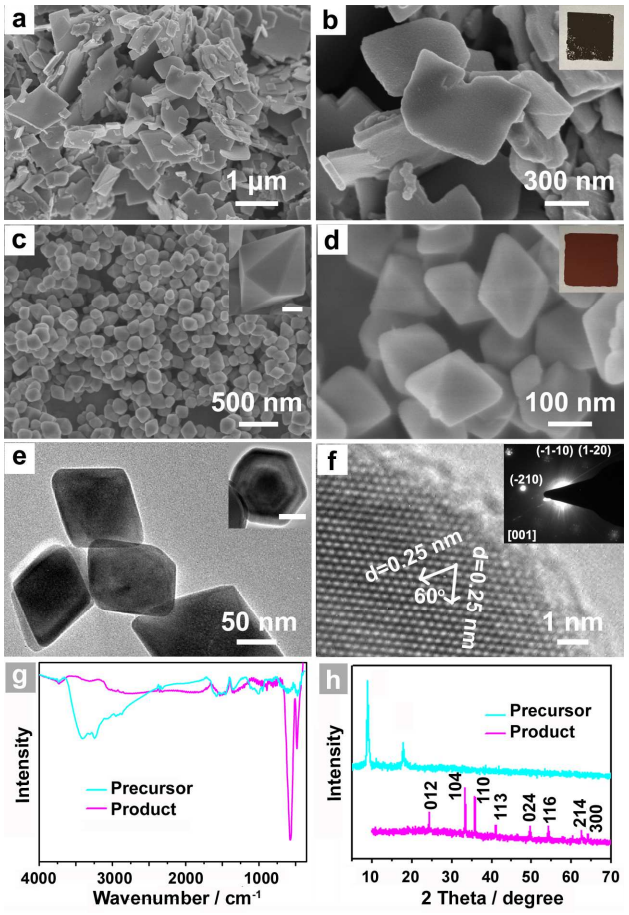

Fig. 1 (a, b) SEM images and photograph (inset) of the inorganic-organic hybrid FeS-DETA nanosheets. (c, d) SEM images and photograph (inset) of the dodecahedral α-Fe_2O_3（inset, scale bars is 50 nm). (e) side view and top view (inset, scale bar is 50 nm) TEM image of the dodecahedral α-Fe_2O_3. (f) HRTEM image of the dodecahedral α-Fe_2O_3 and the corresponding SAED pattern from the [001] zone axis (inset). (g, h) FTIR spectra (g) and XRD patterns (h) of the inorganic-organic hybrid FeS-DETA nanosheets (cyan line) and dodecahedral α-Fe_2O_3 (magenta line).

3. Results and discussion

The FeS-DETA hybrid nanosheets were prepared by a facile hydrothermal reaction. Fig. 1a and 1b display the representative scanning electron microscopy (SEM) images of the FeS-DETA hybrid nanostructures, showing a typical 2D sheet-like morphology with a lateral size distribution of 200~1500 nm and a thickness of 50-100 nm. As shown in Fig. 1h, powder X-ray diffraction (PXRD) pattern shows that the emergence of diffraction peaks are similar to the reported FeS-amine precursors.[60,61] The Fourier transform infrared spectroscopy (FTIR) spectra (Fig. 1g, cyan line) and energy-dispersive X-ray spectroscopy (EDS) analysis (Fig. S1, ESI†) further identify them as the inorganic-organic hybrid nanostructures.

The single-crystalline dodecahedral α-Fe_2O_3 was obtained through a simple hydrothermal treatment of as-obtained FeS-DETA hybrid nanosheets. SEM images show their dodecahedral morphological feature with a lateral size of 100~300 nm (Fig. 1c and 1d). Transmission electron microscopy (TEM) images of the products displayed in Fig. 1e clearly confirm the dodecahedral morphology from side view and top view (inset). Representative high-resolution TEM (HRTEM) image and the associated selected area electron diffraction (SAED) pattern in the inset of Fig. 1f reveal the single crystalline structure of the dodecahedral α-Fe_2O_3. The HRTEM image shows the crystal plane spacings are 0.25 nm, which can be index to {110} or {1-20} lattice spacing of the rhombohedral hematite. As shown in Fig. 1h, all the diffraction peaks from the PXRD pattern can be attributed to the rhombohedral α-Fe_2O_3 (JCPDS 33-0664). No any other peak can be observed in XRD pattern, indicating the high purity of the as-obtained dodecahedral α-Fe_2O_3. FTIR spectra further confirm the transformation from the inorganic-organic FeS-DETA hybrid nanosheets into the inorganic α-Fe_2O_3 (Fig 1g). The photographs in the insets of Fig. 1b and 1d also clearly show the change from the precursor to the product. EDS spectrum and thermogravimetric (TG) analysis demonstrate the composition and high purity of the α-Fe_2O_3 samples (Fig. S2 and Fig. S4 ESI†).

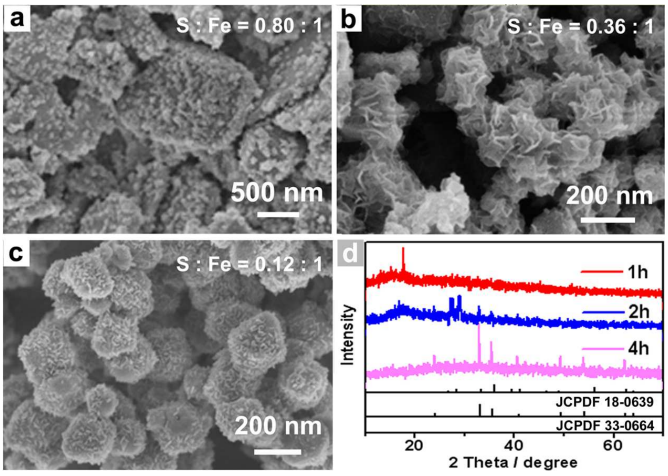

Fig. 2 (a,b,c)SEM image and (d) XRD spectra of the intermediates collected after the reaction proceeded for different times:(a) 1 h, (b) 2 h, (c) 4 h.

To clarify the formation mechanism of the dodecahedral α-Fe_2O_3, SEM, EDS and XRD were used to characterize the intermediates collected at different reaction stages (Fig. 2). At the early stage (Fig. 2a), the FeS-DETA hybrid nanosheets became rough gradually. When the anion-exchange reaction proceeded for another one hour (2 h, Fig. 2b), these small nanoparticles regrew and became small 2D nanosheets. The appearance of nanosheet intermediates could be attributed to the formation of layered FeOOH.[57] The assumption was further confirmed by the analysis of XRD patterns. As shown in Fig. 2d, the peaks of precursor became very weaker, some peaks of FeOOH (JCPDS 18-0639) could be observed as the reaction proceeded for 2 h. When the reaction time was increased to 4h, the dodecahedral crystals with some nanosheets on the surface (Fig. 2c) appeared. XRD pattern in Fig. 2d revealed that the intermediate was mostly α-Fe_2O_3 (JCPDS 33-0664). With the increasing reaction time, the dodecahedral α-Fe_2O_3 crystals with smooth surface were eventually produced (Fig. 1c and 1d). And EDS analysis (Fig. 2a, b, c and Fig. S1-3, ESI†) disclosed that the ratio of S:Fe experienced a decreasing and disappearing process. On the basis of these results, we propose the transformation mechanism of FeS-DETA sheets into dodecahedral α-Fe_2O_3 involving the anion-exchange reaction of inorganic-organic hybrid nanosheets and the dissolution of DETA, as displayed in Scheme 1. Initially, S^{2-} ions are slowly exchanged by the OH^- ions from water accompanied by the dissolution of DETA. Then, the Fe^{2+} ions are subsequently oxidized by the oxygen in the solution to form FeOOH. Finally, the dodecahedral α-Fe_2O_3 crystals appear and become smoothly in the following reaction process. The reactions involved are shown below.

$$\text{FeS-DETA} + 3OH^- \xrightarrow{[O]} \text{FeOOH+DETA+}S^{2-}\text{+}H_2O \xrightarrow{\triangle} \alpha\text{-}Fe_2O_3$$

The introduction of DETA as amine is a key factor. Firstly, it is important to employ FeS-amine inorganic-organic hybrid nanosheets to enhance productivity of the dodecahedral α-Fe_2O_3. In the case of using pure inorganic FeS nanosheets or $FeSO_4 \cdot 7H_2O$ as the precursor, the proportion of the dodecahedral α-Fe_2O_3 in the final products is very low (Fig. S5-8, ESI†). Then DETA as amine in the inorganic-organic hybrid nanosheets is also very important for the uniform of the products (Fig. S9 and S10, ESI†). The uniform of the products is poor in the case of FeS-triethylenetetramine (FeS-TETA) as precursor. Secondly, the alkaline DETA played a vital role in the following transformation of the dodecahedral α-Fe_2O_3 by adjusting the pH of the system to 10 (Fig. S11a, ESI†). When the pH value was adjusted to 7, there's almost no objective products. Without the addition of DETA, the majority of the products are even changed into nanocubes or octahedrons (Fig. S11b and S11c, ESI†). Furthermore, the release of DETA in the following transformation is also very important (Fig. S11d, ESI†). When the dissolution of DETA is totally suppressed, the dodecahedral α-Fe_2O_3 can't be obtained, revealing that the addition of DETA can both facilitate the formation of dodecahedral morphology and the adjustment of suitable pH value.

With the stable dodecahedral α-Fe_2O_3 in hand, we tested their optical absorption properties with UV-vis spectroscopy and PEC activity under visible light illumination (λ > 420 nm) in the electrolyte of 1.0 M KOH (pH = 13.6). For comparison, the commercial α-Fe_2O_3 nanoparticles were also evaluated. As presented in Fig. S9, ESI†, commercial α-Fe_2O_3 nanoparticles (C-hematite) also show small size and uniform morphology. It can be seen from the UV-vis diffuse reflectance spectra that both C-hematite and D-hematite have similar bandgap (*Eg*) of ca. 2.0 eV so that almost all UV light and a large part of the visible light can be employed, while D-hematite still owns stronger absorption ability when compared with C-hematite in the visible region (Fig 3a). To test their PEC performance, I-V curves have been measured under visible light illumination (λ > 420 nm) and in the dark (Fig 3b). In the polarization curves for oxygen evolution reaction (OER), the photocurrent of D-hematite nanostructures (3.06 mA cm^{-2}) is almost four times larger than the C-hematite (0.77 mA cm^{-2}) at the potential of 1.6V versus reversible hydrogen electrode (RHE). Fig. 3c displays the photocurrent responses of D-hematite and C-hematite are prompt, steady and reproducible. Photocurrent-time courses of D-hematite is presented in Fig. 3d, suggesting no obvious decrease of photocurrent in a 10 h test. The electrochemical impedance spectroscopy (EIS) (Fig. S10, ESI†) shows that D-hematite exhibits smaller impedance than C-hematite. The enhanced PEC activity of the D-hematite may be attributed to its unique morphological and structural features. To prove the advantage of the unique dodecahedral morphology, the I-V curves of the samples synthesized using FeS-TETA precursors are also examined. These polarization curves for OER show the photoelectrochemical activities of the dodecahedral samples synthesized using FeS-DETA precursors and FeS-TETA precursors are better than the commercial hematite and synthetic cubic hematite (Fig S14). Firstly, the D-hematite nanostructures harvest more visible light than C-hematite as shown in Fig 3a. The D-hematite from the FeS-DETA precursors may show better PEC activity than that from the FeS-TETA precursors considering the smaller size. What's more, the photocatalytic activity trend of exposed facets are in the order of {110}>{012}>>{001}.[35] The special dodecahedral nanostructures can offer a huge number of {110} facets according to the HRTEM image (Fig. 1f) for exhibiting better photoactivity while the dominant facets of cubic hematite is {012}.[35,45] Secondly, the D-hematite with large fraction of uncoordinated surface atoms can usually supply high density of catalytic active sites.[53] Thirdly, good crystallinity of D-hematite is helpful for the quick charge transfer of the photogenerated carriers.[3] We expect that the PEC activity of such dodecahedral α-Fe_2O_3 can be further improved by surface treatment and the decoration of co-photocatalysts or dopants.

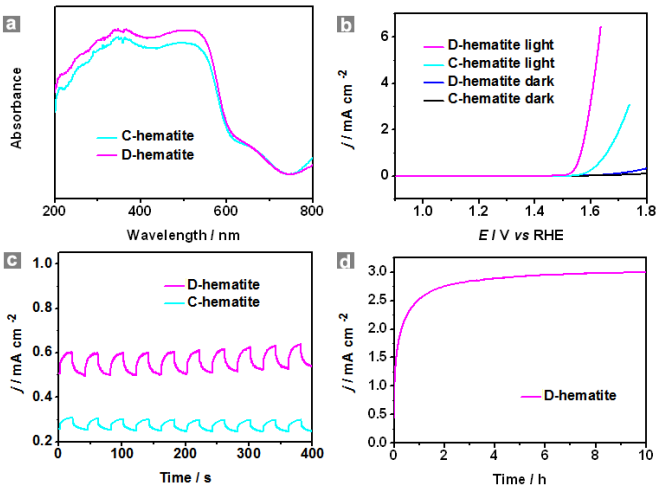

Fig. 3 The PEC performances of the dodecahedral α-Fe_2O_3 (D-hematite, magenta line) and commercial α-Fe_2O_3 nanoparticles (C-hematite, cyan line): (a) UV-Vis diffuse reflectance spectra; (b) *iR*-corrected polarization curves for oxygen evolution reaction (OER) under visible light illumination (λ > 420 nm) and in the dark(D-hematite, blue line. C-hematite, black line) with scan speed at 10mV s^{-1}; (c) Photocurrent response at an applied bias potential of 1.6 V *vs* RHE in 1.0 M KOH aqueous solution under repeated on/off cycles of visible light illumination (λ > 420 nm); (d) Photocurrent-time curve at an applied bias potential of 1.6 V *vs* RHE under visible light illumination (λ > 420 nm) in 1.0 M KOH .

4. Conclusion

In summary, dodecahedral α-Fe_2O_3 nanostructures have been successfully prepared via a simple and cost-effective DETA-assisted hydrothermal treatment of the inorganic-organic hybrid FeS-DETA 2D nanosheet precursors. It is found that the presence of DETA is mainly responsible for the formation of the dodecahedral α-Fe_2O_3. These dodecahedral α-Fe_2O_3 shows enhanced PEC activity and good stability under visible light irradiation (λ > 420 nm) in the presence of 1.0 M KOH as electrolyte. In addition to their promising application as the efficient PEC water splitting, the dodecahedral α-Fe_2O_3 may find broad applications in the fields of organic catalysis,[63] water treatment[35] and dye-sensitized solar cells[64].

Acknowledgements

This work was financially supported by the National Natural Science Foundation of China (No. 21422104 and No. 21373149) and the Innovation Foundation of Tianjin University.

Notes and references

Department of Chemistry, School of Science, Tianjin University, and Collaborative Innovation Center of Chemical Science and Engineering (Tianjin), Tianjin 300072, China. E-mail: bzhang@tju.edu.cn

† Electronic supplementary information (ESI) available: Experimental instruments and additional characterization results. See DOI: 10.1039/c000000x/

1 M. Gratzel, *Nature*, 2001, **414**, 338.

2 M. G. Walter, E. L. Warren, J. R. McKone, S. W. Boettcher, Q. Mi, E. A. Santori and N. S. Lewis, *Chem. Rev.*, 2010, **110**, 6446.

3 Z. Li, W. Luo, M. Zhang, J. Feng and Z. Zou, *Energy Environ. Sci.*, 2013, **6**, 347.
4 A. Fujishima and K. Honda, *Nature*, 1972, **238**, 37.
5 H. M. Chen, C. K. Chen, R. S. Liu, L. Zhang, J. Zhang and D. P. Wilkinson, *Chem. Soc. Rev.*, 2012, **41**, 5654.
6 F. E. Osterloh, *Chem. Mater.*, 2007, **20**, 35.
7 F. E. Osterloh, *Chem. Soc. Rev.*, 2013, **42**, 2294.
8 L. Shang, T. Bian, B. Zhang, D. Zhang, L. Wu, C. H. Tung, Y. Yin, and T. Zhang, *Angew. Chem. Int. Ed.*, 2014, **53**, 250.
9 C. Zhou, Y. Zhao, L. Shang, Y. Cao, L. Z. Wu, C. H. Tung and T. Zhang, *Chem. Commun.*, 2014, **50**, 9554.
10 T. Bian, L. Shang, H. Yu, M. T. Perez, L. Z. Wu, C. H. Tung, Z. Nie, Z. Tang and T. Zhang, *Adv. Mater.*, 2014, **26**, 5613.
11 Y. Lin, G. Yuan, S. Sheehan, S. Zhou and D. Wang, *Energy Environ. Sci.*, 2011, **4**, 4862.
12 K. Sivula, F. L. Formal, and M. Gratzel, *ChemSusChem.*, 2011, **4**, 432.
13 R. H. Goncalves, B. H. R. Lima and E. R. Leite, *J. Am. Chem. Soc.*, 2011, **133**, 6012.
14 D. K. Zhong, M. Cornuz, K. Sivula, M. Gratzel and D. R. Gamelin, *Energy Environ. Sci.*, 2011, **4**, 1759.
15 T. K. Townsend, E. M. Sabio, N. D. Browning and F. E. Osterloh, *Energy Environ. Sci.*, 2011, **4**, 4270.
16 D. A. Wheeler, G. Wang, Y. Ling, Y. Li and J. Z. Zhang, *Energy Environ. Sci.*, 2012, **5**, 6682.
17 N. J. Cherepy, D. B. Liston, J. A. Lovejoy, H. Deng and J. Z. Zhang, *J. Phys. Chem. B*, 1998, **102**, 770.
18 A. G. Joly, J. R. Williams, S. A. Chambers, G. Xiong W. P. Hess and D. M. Laman, *J. Appl. Phys*.,2006, **99**, 053521.
19 C. Y. Cummings, F. Marken, L. M. Peter, K. G. U. Wijayantha and A. A. Tahir, *J. Am. Chem. Soc.*, 2012, **134**, 1228.
20 B. Klahr, S. Gimenez, F. Fabregat-Santiago, T. Hamann and J. Bisquert, *J. Am. Chem. Soc.*, 2012, **134**, 4294.
21 G. Wang, Y. Ling and Y. Li, Nanoscale, 2012, **4**, 6682.
22 K. Sivula, R. Zboril, F. L. Formal, R. Robert, A. Weidenkaff, J. Tucek, J. Frydrych, and M. Gratzel, *J. Am. Chem. Soc.*, 2010, **132**, 7436.
23 A. Duret and M. Gratzel, *J. Phys. Chem. B*, 2005, **109**, 17184.
24 N. T. Hahn, H. Ye, D. W. Flaherty, A. J. Bard, and C. B. Mullins, *ACS Nano*, 2010, **4**,1977.
25 A. Kay, I. Cesar, and M. Gratzel, *J. Am. Chem. Soc.*, 2006, **128**, 15714.
26 J. S. Xu and Y. J. Zhu, *CrystEngComm*, 2012, **14**, 2702.
27 U. Bjorksten, J. Moser, and M. Gratzel, *Chem. Mater.* 1994, **6**, 858.
28 X. Mou, X. Wei, Y. Li and W. Shen, *CrystEngComm*, 2012, **14**, 5107.
29 N. K. Chaudhari, H. C. Kim, M. S. Kim, J. Park and J. S. Yu, *CrystEngComm.*, 2012, **14**, 2024.
30 L. Vayssieres, C. Sathe, S. M. Butorin, D. K. Shuh, J. Nordgren and J. Guo, *Adv. Mater.*, 2005, **17**, 2320.
31 L. Vayssieres, N. Beermann, S. E. Lindquist and A. Hagfeldt, *Chem. Mater.*, 2001, **13**, 233.
32 M. Rachel, R. Mahfujur, J. M. D. MacElroy and C. A.Wolden, *ChemSusChem*, 2011, **4**, 474.
33 F. Meng, S. A. Morin and S. Jin, *J. Am. Chem. Soc.*, 2011, **133**, 8408.
34 S. K. Mohapatra, S. E. John, S. Banerjee and M. Misra, *Chem. Mater.*, 2009, **21**, 3048.
35 X. Zhou, J. Lan, G. Liu, K. Deng, Y. Yang, G. Nie, J. Yu and L. Zhi, *Angew. Chem. Int. Ed.*, 2012, **51**, 178.
36 S. Xiong, J. Xu, D. Chen, R. Wang, X. Hu, G. Shen and Z. L. Wang, *CrystEngComm*, 2011, **13**, 7114.
37 L. Li, H. B. Wu, L. Yu, S. Madhavi and X. W. Lou, *Adv. Mater. Interfaces*, 2014, **1**, 1400050.
38 W. Cheng, J. He, T. Yao, Z. Sun, Y. Jiang, Q. Liu, S. Jiang, F. Hu, Z. Xie, B. He, W. Yan and S. Wei, *J. Am. Chem. Soc.* 2014, **136**, 10393.
39 M. Lin, H. R. Tan, J. P. Y. Tan and S. Bai, *J. Phys. Chem. C*, 2013, **117**, 11242.
40 L. S. Zhong, J. S. Hu, H. P. Liang, A. M. Cao, W. G. Song and L. J. Wan, *Adv. Mater.*, 2006, **18**, 2426.
41 S. B. Wang, Y. L. Min and S. H. Yu, *J. Phys. Chem. C*, 2007, **111**, 3551.
42 X. Liang, X. Wang, J. Zhuang, Y. Chen, D. Wang, and Y. Li, *Adv. Funct. Mater.*, 2006, **16**, 1805.
43 B. Jia and L. Gao, *Cryst. Growth & Des.*, 2008, **8**, 1372.
44 L. Zhang, H. B. Wu, S. Madhavi, H. H. Hng and X. W. Lou, *J. Am. Chem. Soc.*, 2012, **134**, 17388.
45 W. Wu, R. Hao, F. Liu, X. Su and Y. Hou, *J. Mater. Chem. A*, 2013, **1**, 6888.
46 Y. Liang, L. Shang, T. Bian, C. Zhou, D. Zhang, H. Yu, H. Xu, Z. Shi, T. Zhang, L. Z. Wu and C. H. Tung, *CrystEngComm.*, 2012, **14**, 4431.
47 J. Yang and T. Sasaki, *Cryst. Growth Des.*, 2010, **10**, 1233.
48 Y. Xu, H. Wang, Y. Yu, L. Tian, W. Zhao and B. Zhang, *J. Phys. Chem. C*, 2011, **115**, 15288.
49 S. Inamdar, H. S. Choi, M. S. Kim, K. Chaudhari and J. S. Yu, *CrystEngComm.*, 2012, **14**, 7009.
50 W. J. Li, E. W. Shi, W.Z. Zhong and Z.W. Yin, *J. Cryst. Growth*, 1999, **203**, 186.
51 Y. Jun, J. Choi and J. Cheon, *Angew. Chem. Int. Ed.*, 2006, **45**, 3414.
52 Z. Zhang, B. Xu and Xun Wang, *Chem. Soc. Rev.*, 2014, DOI: 10.1039/C3CS60389J.
53 J. Yin, Z. Yu, F. Gao, J. Wang, H. Pang and Q. Lu, *Angew. Chem. Int. Ed.*, 2010, **49**, 6328.
54 Y. Yang, H. Ma, J. Zhuang and X. Wang, *Inorg. Chem.*, 2011, **50**, 10143.
55 B. Lv, Z. Liu, H. Tian, Y. Xu, D. Wu and Y. Sun, *Adv. Funct. Mater.*, 2010, **20**, 3987.
56 R. Liu, Y. Jiang, H. Fan, Q. Lu, W. Du and F. Gao, *Chem. Eur. J.*, 2012, **18**, 8957;
57 T. K. Van, H. G. Cha, C. K. Nguyen, S. W. Kim, M. H. Jun and Y. S. Kang, *Cryst. Growth Des.*, 2012, **12**, 862.
58 X. Li, W. Wei, S. Wang, L. Kuai and B. Geng, *Nanoscale.*, 2011, **3**, 718.
59 X. Liu, J. Zhang, S. Wu, D. Yang, P. Liu, H. Zhang, S. Wang, X Yao, G. Zhu and H. Zhao, *RSC Adv.*, 2012, **2**, 6178.
60 Z. Zang, H. B. Yao, Y. X. Zhou, W. T. Yao and S. H. Yu, *Chem. Mater.*, 2008, **20**, 4749.
61 W. T. Yao, H. Z. Zhu, W. G. Li, H. B. Yao, Y. C. Wu and S. H. Yu, *ChemPlusChem.*, 2013, **78**, 723.
62 X. L. Fang, Y. Li, C. Chen, Q. Kuang, X. Z. Gao, Z. X. Xie, S. Y. Xie, R. B. Huang and L. S. Zheng, *Langmuir*, 2010, **26**, 2745.

63 M. Shokouhimehr, Y. Piao, J. Kim, Y. Jang and T. Hyeon, *Angew. Chem. Int. Ed.*, 2007, **46**, 7039.
64 Y. Hou, D. Wang, X. H. Yang, W. Q. Fang, B. Zhang, H. F. Wang, G. Z. Lu, P. Hu, H. J. Zhao and H. G. Yang, *Nat. Commun.*, 2013, **4**, 1583.

A Table of Contents Entry

Colour graphic:

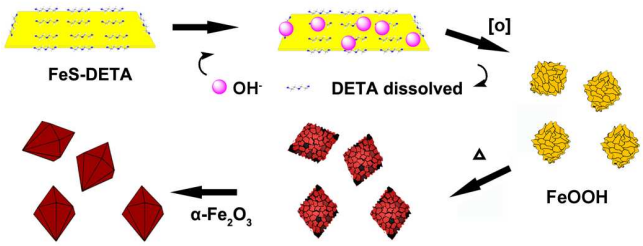

Text:

A facile diethylenetriamine-assisted protocol is developed to prepare dodecahedral α-Fe_2O_3 nanocrystals, which exhibit efficient photoelectrocatalytic water splitting activity.